



PII S0038-1098(96)00136-6

## SELF-CONSISTENT TIGHT-BINDING CALCULATIONS OF ELECTRONIC AND OPTICAL PROPERTIES OF SEMICONDUCTOR NANOSTRUCTURES

Aldo Di Carlo, Sara Pescetelli, Marco Paciotti and Paolo Lugli

INFN-Dipartimento di Ingegneria Elettronica, Università di Roma "Tor Vergata", 00133 Roma, Italy

Martin Graf

Walter Schottky Institut, TU-München, 85748 Garching, Germany

(Received 7 February 1996; accepted 4 March 1996 by E. Molinari)

Optical properties and electronic states of semiconductor nanostructures are calculated by using tight-binding models which account for valence band mixing, strain and external applied potentials in a self-consistent fashion. An appropriate formulation of the optical susceptibility in the tight-binding basis is given without introducing any additional parameters. Results for strained and unstrained systems are given. Copyright © 1996 Published by Elsevier Science Ltd

Keywords: Semiconductors, nanostructures, electronic band structure, optical properties.

## 1. INTRODUCTION

Electronic and optical properties of semiconductor nanostructures based on homo- and heterojunctions have been investigated theoretically by means of a variety of tools. These range from *ab-initio* approaches [1], which are very precise but require a large computational effort and, consequently, are limited only to very small nanostructures, to approximate but easy-to-handle and fast methods such as for example those based on the envelope function approximation (EFA) [2]. In its simplest form, the EFA leads to the evaluation of the energy levels of nanosystems by simply solving a one-electron Schrödinger equation where each semiconductor is described in terms of effective masses and band edges. Such an approach, and its generalizations, have been very successful [2], even though several problems cannot be handled easily within the EFA context. Among them, e.g., band mixing, indirect gap, and strain [3–6]. The empirical tight binding method (TB) [3, 4, 6, 7] has been shown to be a valid alternative to EFA, since it improves the physical content in the description of the nanostructure with respect to EFA, without requiring a much higher computational effort. So far, however, TB has been mainly used in the calculation of the electronic properties of nanostructures without tak-

ing into account self-consistent charge redistribution, which is an important requirement when we deal with real systems. In this paper we will show that the tight-binding method can be used in a self-consistent fashion and we demonstrate that TB is well suited for the calculation of optical and electronic properties of realistic nanostructures. By using a recently developed theory [8] we also show how to define the susceptibility tensor, without requiring periodic boundary conditions. This makes the method suitable for nanosystems where the translational symmetry is broken at least in one direction.

## 2. SELF-CONSISTENCY AND SUSCEPTIBILITY TENSOR

In this section we discuss the self-consistent tight-binding model and we introduce the expression for the imaginary part of the susceptibility tensor in a system where the symmetry is broken in one direction for example the growth axis (*z*). The wave function  $|E, \mathbf{k}_{||}\rangle$  can be written as linear combination of planar Bloch sums,  $|\alpha, m\rangle$  [9]

$$|E, \mathbf{k}_{||}\rangle = \sum_{\alpha, m} C_{\alpha, m}(\mathbf{k}_{||}, E) |\alpha, m\rangle \quad (1)$$

with

$$|\alpha, m\rangle = \frac{1}{\sqrt{N}} \sum_{\mathbf{R}_{\alpha}^m} e^{i\mathbf{k}_{\parallel} \cdot \mathbf{R}_{\alpha}^m} |\alpha, \mathbf{R}_{\alpha}\rangle, \quad (2)$$

where  $|\alpha, \mathbf{R}_{\alpha}\rangle$  is a localized orbital,  $\mathbf{k}_{\parallel}$  is the in-plane wave vector and  $N$  is the number of unit cells in the atomic plane. The subindex  $\alpha$  refer both to the basis atom index and to the atomic orbital index. The lattice vector,  $\mathbf{R}_{\alpha} = \mathbf{R} + \mathbf{v}_{\alpha}$ , (where  $\mathbf{v}$  is the basis atom displacement), can be written as a sum of two terms  $\mathbf{R}_{\alpha} = m\mathbf{d} + \mathbf{R}_{\alpha\parallel}^m$  with an integer  $m$ . There,  $\mathbf{d}$  is a vector parallel to the growth direction with module equal to the distance between two atomic planes and  $\mathbf{R}_{\alpha\parallel}^m$  is a vector on the  $m$ -th atomic plane. For a given  $\mathbf{k}_{\parallel}$ , the eigenstates  $E$  are calculated by solving the secular equation  $(H + V_H)|E, \mathbf{k}_{\parallel}\rangle = E|E, \mathbf{k}_{\parallel}\rangle$  where  $H$  is the system tight-binding hamiltonian and  $V_H$  is the Hartree potential. In order to calculate electronic and optical properties for real heterosystems, the presence and possible rearrangement of free charges has to be taken into account. The influence of the electronic charge rearrangement can be included at a Hartree level by solving the Poisson equation for the Hartree potential,  $d^2V_H/dz^2 = -\rho(z)/\epsilon$ , where  $\epsilon$  is the static dielectric constant. The charge density  $\rho(z)$  is defined by the square of the wave function averaged over a layer  $z$  and weighted by the Fermi function  $f(E)$ :

$$\rho(z) = \frac{e}{(2\pi)^2} \int d\mathbf{k}_{\parallel} \sum_n |\Psi_{n,\mathbf{k}_{\parallel}}|^2 f(E_n), \quad (3)$$

where  $e$  is the electron charge and  $n$  labels the energy levels for a given  $\mathbf{k}_{\parallel}$ . A full  $\mathbf{k}_{\parallel}$  integration is performed in the 2D Brillouin zone by using the special k-points technique in the irreducible wedge [10]. The convergence of this integration has been obtained by using 9 special points with  $|\mathbf{k}_{\parallel}| \leq 0.062\pi/a$ . Poisson and Schrödinger equation in the tight-binding representation are iteratively solved until convergence is reached. Open-chain (infinite well) boundary condition is used for Schrödinger's equation. In order to avoid influences on calculated electronic levels, boundaries are chosen far away from the nanostructure region where the density of conduction electrons or valence holes is high. Although a better choice for the boundary condition is provided by complex band structure states as explained in Ref. [9], for all the situations discussed here the open chain condition represents a valid and simple choice. In order to speed up the self-consistent algorithm we have introduced a hybrid method to diagonalize the tight-binding hamiltonian which uses a standard (LAPACK [11]) routine to calculate eigenvalues and an inverse iteration scheme to calculate eigenvectors.

When optical properties are of interest, one can make use of the Kubo formula to define the suscep-

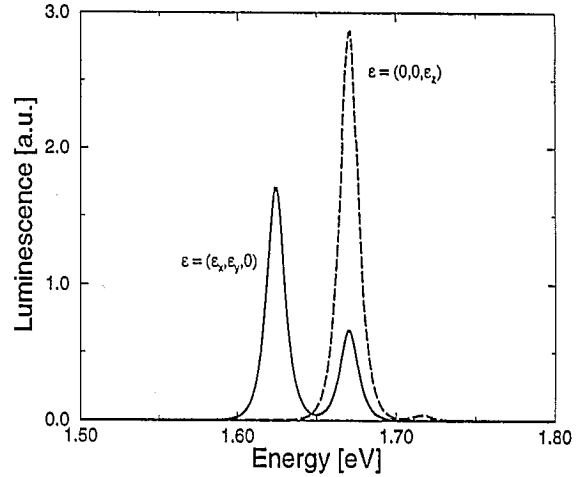


Fig. 1. Photoluminescence spectra of the  $\text{Al}_{0.3}\text{Ga}_{0.7}\text{As}/\text{GaAs}/\text{Al}_{0.3}\text{Ga}_{0.7}\text{As}$  quantum well with 28 Å well width. Both polarizations, perpendicular (solid line) and parallel (dashed line) to the  $z$  direction, are shown.

tibility tensor which is related to the current-current response function of the electromagnetic perturbation [8]. For the imaginary part we obtain:

$$\begin{aligned} \text{Im } \chi_{i,i'}(\alpha, m; \alpha', m'; \omega) &= \frac{1}{\omega^2 S} \sum_{E, E', \mathbf{k}_{\parallel}} [f(E) - f(E')] \delta(\hbar\omega + E - E') \\ &\times \langle E, \mathbf{k}_{\parallel} | J_i^{(0)}(\alpha, m) | E', \mathbf{k}_{\parallel} \rangle \\ &\times \langle E', \mathbf{k}_{\parallel} | J_{i'}^{(0)}(\alpha', m') | E, \mathbf{k}_{\parallel} \rangle. \end{aligned} \quad (4)$$

Here,  $S$  is the transverse area of the primitive cell. The basis set for the evaluation of the current operator is given by the system wave functions  $|E, \mathbf{k}_{\parallel}\rangle$  which can be either the scattering states [9] or the limited wave functions, depending on the adopted boundary conditions, i.e., complex bulk states or open chain, respectively. Equation 4 extends the result of Ref. [8] to the case in which symmetry is lost along one direction. The matrix elements of the current operator can be expressed as:

$$\begin{aligned} \langle E, \mathbf{k}_{\parallel} | \mathbf{J}^{(0)}(\alpha, m) | E', \mathbf{k}_{\parallel} \rangle &= \frac{S}{N} \sum_{\substack{\alpha', m' \\ \alpha'', m''}} C_{\alpha', m'}^*(E, \mathbf{k}_{\parallel}) C_{\alpha'', m''}(E', \mathbf{k}_{\parallel}) \\ &\times \sum_{\mathbf{R}_{\alpha\parallel}^m, \mathbf{R}_{\alpha'\parallel}^{m'}, \mathbf{R}_{\alpha''\parallel}^{m''}} e^{i\mathbf{k}_{\parallel} \cdot (\mathbf{R}_{\alpha''\parallel}^{m''} - \mathbf{R}_{\alpha'}^{m'})} \\ &\times \langle \alpha', \mathbf{R}_{\alpha'} | \mathbf{j}^{(0)}(\alpha, \mathbf{R}_{\alpha}) | \alpha'', \mathbf{R}_{\alpha''} \rangle, \end{aligned} \quad (5)$$

where the current operator between localized orbitals  $\langle \alpha', \mathbf{R}_{\alpha'} | \mathbf{j}^{(0)}(\alpha, \mathbf{R}_{\alpha}) | \alpha'', \mathbf{R}_{\alpha''} \rangle$  can be evaluated by writing the tight-binding hamiltonian in the presence of an electromagnetic field. By relating the variation

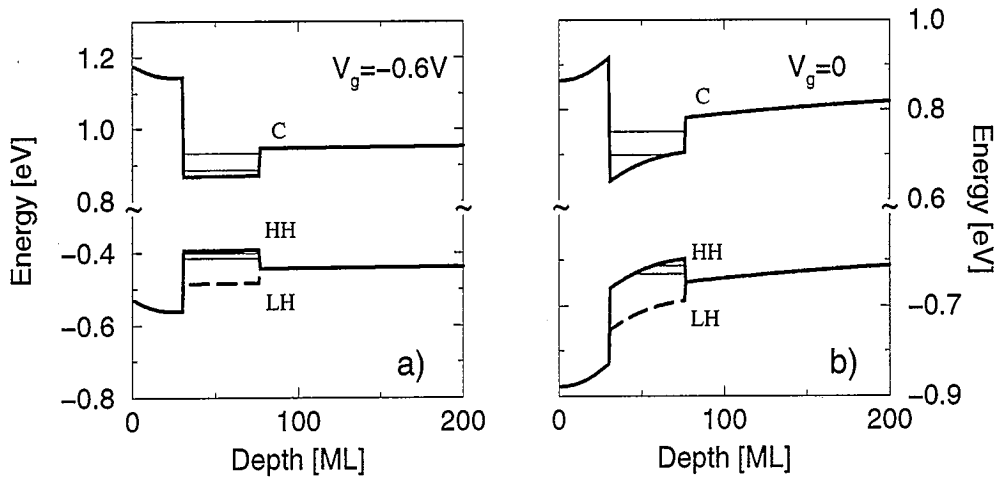


Fig. 2. Self consistent band edge profile of the  $\text{Al}_{0.2}\text{Ga}_{0.8}\text{As}/\text{In}_{0.15}\text{Ga}_{0.85}\text{As}/\text{GaAs}$  pseudomorphic structure at applied gate voltages of -0.6 V (a) and 0.0 V (b). The depth is measured in monolayers [ML].

of the hamiltonian to the variation of the vector potential [8] one obtains

$$\begin{aligned} & \langle \alpha', \mathbf{R}_{\alpha'} | j^{(0)}(\alpha, \mathbf{R}_{\alpha}) | \alpha'', \mathbf{R}_{\alpha''} \rangle \\ &= \frac{ie}{2\hbar dS} t_{\alpha', \alpha''}(\mathbf{R}_{\alpha'} - \mathbf{R}_{\alpha''}) [\mathbf{R}_{\alpha'} - \mathbf{R}_{\alpha''}] \quad (6) \\ & \times \left\{ \delta_{\alpha', \alpha''} + \delta_{\alpha'', \alpha'} \right\}, \end{aligned}$$

where  $t_{\alpha', \alpha''}(\mathbf{R}_{\alpha'} - \mathbf{R}_{\alpha''}) = \langle \alpha', \mathbf{R}_{\alpha'} | H | \alpha'', \mathbf{R}_{\alpha''} \rangle$  is the tight-binding hopping matrix element.

### 3. RESULTS

As a first application, we calculate the photoluminescence spectra of a squared AlGaAs-GaAs-AlGaAs quantum well (QW). A  $sp^3s^*$  model [12] with spin-orbit interaction has been used for the tight-binding hamiltonian. In order to emphasize effects related to polarization and symmetry, we have assumed that electrons in the quantized levels of the conduction band are close to  $\mathbf{k}_{\parallel} = 0$  and that only few quantized levels of the valence band are empty. An additional broadening of 5 meV has been introduced to account for the finite linewidth of the photoluminescence spectra.

In Fig. 1 we distinguish between two different polarizations of the emitted light. We notice that the transition  $E_1 \rightarrow HH_1$  between the first conduction level and the first heavy hole level is forbidden for light polarized in the  $z$  direction, while the transition  $E_1 \rightarrow LH_1$  between the first conduction level and the first light hole level shows a predominant contribution of the  $z$ -polarized light. This is in agreement within the results obtained in the EFA [2]. The intensity peak ratio between  $E_1 \rightarrow HH_1$  and  $E_1 \rightarrow LH_1$  for parallel polarizations is 2.587, to compare with 3 obtained with EFA, while the intensity peak ratio for the two polar-

izations of the transition  $E_1 \rightarrow LH_1$  is 0.595 in our method and 0.75 in EFA. These differences are an evidence of band mixing effects in the valence band and band non-parabolicity, both an inherent feature of the tight-binding approach.

The second example refers to a pseudomorphic structure consisting of a 360 Å n-doped ( $n=10^{18}\text{cm}^{-3}$ )  $\text{Al}_{0.2}\text{Ga}_{0.8}\text{As}$ , 20 Å undoped  $\text{Al}_{0.2}\text{Ga}_{0.8}\text{As}$ , a 265 Å strained well of  $\text{In}_{0.15}\text{Ga}_{0.85}\text{As}$  and a GaAs substrate. Such a modulation-doped structure is typical for PM HEMT's a device of great importance in the microwave field [13]. In this calculation the background charge of the doped region is simply added to the free charge as given by Eq. 3. The self-consistent potential profile of the structure for an applied voltage of -0.6 and 0.0 V is shown in Fig. 2a and 2b, respectively. Strain effects in the InGaAs region, which are taken into account by scaling the hamiltonian matrix elements [14], split the HH and LH valence bands. Here the labels HH and LH refer to the character of the valence band in the growth direction. In the parallel direction the uppermost valence band has a light hole character while the other a heavy hole one. Strain also induces large changes on the effective masses of the valence bands. For the unstrained situation we have  $m_{HH} = 0.4475m_0$  and  $m_{LH} = 0.06481m_0$ , while for bulk  $\text{In}_{0.15}\text{Ga}_{0.85}\text{As}$  strained on GaAs the effective masses are  $m_{HH}[001] = 0.4328m_0$ ,  $m_{LH}[001] = 0.09596m_0$ ,  $m_{LH}[100] = 0.08599m_0$  and  $m_{HH}[100] = 0.1391m_0$ . In the confined system, the hole energy level present a different in-plane mass which depends on the energy. For an applied potential of -0.6 V the first three hole levels effective masses are  $m_{h1}[100] = 0.10092m_0$ ,  $m_{h2}[100] = 0.14799m_0$ ,  $m_{h3}[100] = 0.2421m_0$ , respectively. We observe that carrier confinement induces as a consequence of band non-parabolicity an enhance-

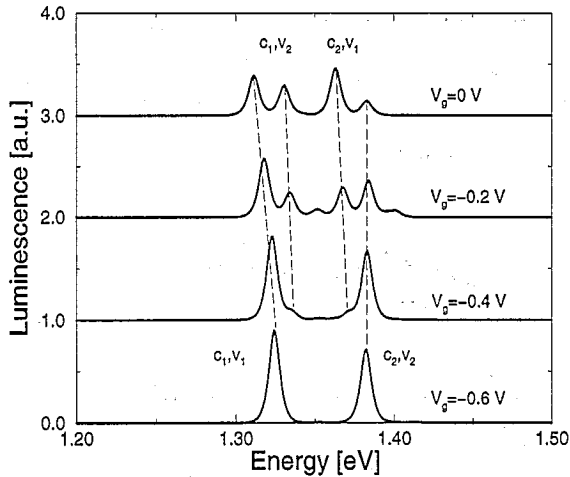


Fig. 3. Photoluminescence spectra of the pseudomorphic structure for several applied voltages. The dashed lines follow the different luminescence peaks.

ment of the effective mass compared to strained bulk material. The calculated photoluminescence spectra for several applied potentials is shown in Fig. 3. Since the HH quantized levels are now above the LH states, the luminescence transitions occur between conduction levels and the heavy hole levels. For an applied voltage of  $-0.6$  V, which correspond to a nearly flat InGaAs band, the main luminescence peaks are related to the  $E_1 \rightarrow HH_1$  and  $E_2 \rightarrow HH_2$  transitions. This is in agreement with the selection rules  $\Delta_{nm} = 0$ , where  $n$  labels the conduction states and  $m$  the valence states [2]. The emitted light is mainly polarized in the in-plane direction since the levels have essentially a heavy-hole character. When the applied potential is reduced, two other peaks form which correspond to the  $E_1 \rightarrow HH_2$  and  $E_2 \rightarrow HH_1$  transitions. Indeed, by decreasing the applied potential, the increasing channel electron density induces a sizable band bending which is responsible for the loss of symmetry (see Fig. 2b) and the transitions  $E_1 \rightarrow HH_2$  and  $E_2 \rightarrow HH_1$  are no longer forbidden. We also notice the presence of a red shift (quantum Stark shift) of the  $E_1 \rightarrow HH_1$  transition due to the presence of an electric field as the applied potential reduces from  $-0.6$  to  $0.0$  V.

In conclusion, we have shown that a self-consistent tight-binding approach can be used to evaluate the

electronic structure and optical properties of semiconductor nanostructures. This represents a further step, with respect to the envelope function model, towards an *ab initio* calculation of such properties.

*Acknowledgements*—We acknowledge the support of the ESPRIT Project NANOPT, of the Deutsche Forschungsgemeinschaft (SFB 348) and of the Bayerische Forschungsverbund (FOROPTO).

## REFERENCES

1. D. M. Wood, S.-H. Wei, and Alex Zunger, *Phys. Rev.* **B37**, 1342 (1988); C. H. Park and K. J. Chang, *Phys. Rev.* **B47**, 12709 (1993).
2. G. Bastard, *Wave mechanics applied to semiconductor heterostructure* (Les Edition de Physique, Les Ulis Cedex, 1988).
3. T.B. Boykin, J.P.A. van der Wagt, and J.S. Harris, *Phys. Rev.* **B43**, 4777 (1991).
4. A. Di Carlo, P. Lugli, *Semicon. Sci. Technol.* **10**, 1673 (1995).
5. A. Zunger, C.-Y. Yeh, L.-W. Wang, S. B. Zang, *Proceedings ICPS-22*, 1763 (1994).
6. J. N. Schulman, Y. C. Chang, *Phys. Rev.* **B31**, 2056 (1985).
7. J. C. Slater, G. F. Koster, *Phys. Rev.* **94**, 1498 (1954); D. W. Bullet, *Solid State Physics*, **35**, 129 (1980); J. A. Majewski, P. Vogl, *The structure of binary compounds* edited by F. R. de Boer and D. G. Pettifor (Elsevier, Amsterdam, 1989).
8. M. Graf and P. Vogl, *Phys. Rev.* **B51**, 4940 (1995).
9. A. Di Carlo, P. Vogl, and W. Pötz, *Phys. Rev.* **B50**, 8358 (1994).
10. S. Froyen, *Phys. Rev.* **B39**, 3168 (1989).
11. E. Anderson, Z. Bai, C. Bischof, J. Demmel, J. Dongarra, J. Du Croz, A. Greenbaum, S. Hammarling, A. McKenney, S. Ostrouchov, D. Sorensen, *LAPACK User's Guide*, (SIAM, Philadelphia, 1992).
12. P. Vogl, H. P. Hjalmarson, J. D. Dow, *J. Phys. Chem. Solids* **44**, 365 (1983).
13. H. Morkoç, H. Unlu, G. Ji, *Principles and Technology of MODFETS*, (John Wiley & Sons, Chichester, 1991).
14. C. Priester, G. Allan, M. Lannoo, *Phys. Rev.* **B37**, 8519 (1988).